Fang *et al.*
Journal of Engineering and Applied Science (2022) 69:95
https://doi.org/10.1186/s44147-022-00144-x

Journal of Engineering and Applied Science

RESEARCH Open Access

Structure and arrangement optimization of non-diagenetic gas hydrate jet crushing nozzles based on CFD simulation

Xiaoyu Fang[1], Xushen Li[1], Lin Zhong[1,2*], Xing Fang[2] and Jiang Lu[1]

*Correspondence:
zhonglin858296@163.com

[1] Southern Marine Science and Engineering Guangdong Laboratory (Zhanjiang), Zhanjiang 440800, Guangdong, China
[2] School of Mechanical Engineering, Southwest Petroleum University, Chengdu 610500, Sichuan, China

Abstract

To optimize the optimal nozzle structure and multiple nozzle arrangement for hydrate jet crushing and to promote the development of solid fluidization extraction technology for shallow unconformity hydrate in China's oceans, the submerged jet flow field of six commonly used nozzle structures in the downhole in-situ jet crushing process was analyzed on the basis of the solid fluidization extraction process in double-layer pipes, and the effect of the jet hole arrangement on the overflow performance of hydrate slurry in the outer annulus of double-layer pipes was also investigated. It was demonstrated that tapered straight nozzles were preferably selected as the nozzle type for hydrate solid fluidization mining process based on jet core stage length, jet energy dissipation rate, and jet fluid axial velocity. In the meantime, the optimum arrangement of the nozzles was preferred on the basis of the annular pressure drop and the flow resistance coefficient, with the number of single circle not higher than 3 and the axial spacing of the nozzles not lower than 50 mm. This study can provide a theoretical basis for nozzle selection and tool design for the solid fluidization jet crushing process of marine unconformable hydrates.

Keywords: Non-diagenetic gas hydrate, Submerged jet, Single nozzle structure optimization, Multiple nozzle arrangement, Over-flow performance

Introduction

Natural gas hydrate (NGH) is a clean energy that has great prospects for development. In comparison with traditional fossil energy sources, NGH have many advantages such as large reserves, high energy density and cleanliness [1, 2, 3, 4, 5]. However, there are still many technical difficulties in the extraction process of NGH. Currently, the most commonly used extraction technology such as depressurization method and heat injection method are prone to serious geological hazards when continuously mined, and lead to environmental disasters. To overcome many process difficulties in NGH extraction, Zhou Shouwei et al. [6] proposed a solid fluidization exploitation method for NGH extraction, which achieves NGH extraction without change the reservoir temperature, pressure, and phase equilibrium, and has the advantages of reservoir protection and low secondary hazards, etc. In May 2017, the success of the first subsea NGH solid

Springer Open

© The Author(s) 2022. **Open Access** This article is licensed under a Creative Commons Attribution 4.0 International License, which permits use, sharing, adaptation, distribution and reproduction in any medium or format, as long as you give appropriate credit to the original author(s) and the source, provide a link to the Creative Commons licence, and indicate if changes were made. The images or other third party material in this article are included in the article's Creative Commons licence, unless indicated otherwise in a credit line to the material. If material is not included in the article's Creative Commons licence and your intended use is not permitted by statutory regulation or exceeds the permitted use, you will need to obtain permission directly from the copyright holder. To view a copy of this licence, visit http://creativecommons.org/licenses/by/4.0/. The Creative Commons Public Domain Dedication waiver (http://creativecommons.org/publicdomain/zero/1.0/) applies to the data made available in this article, unless otherwise stated in a credit line to the data.

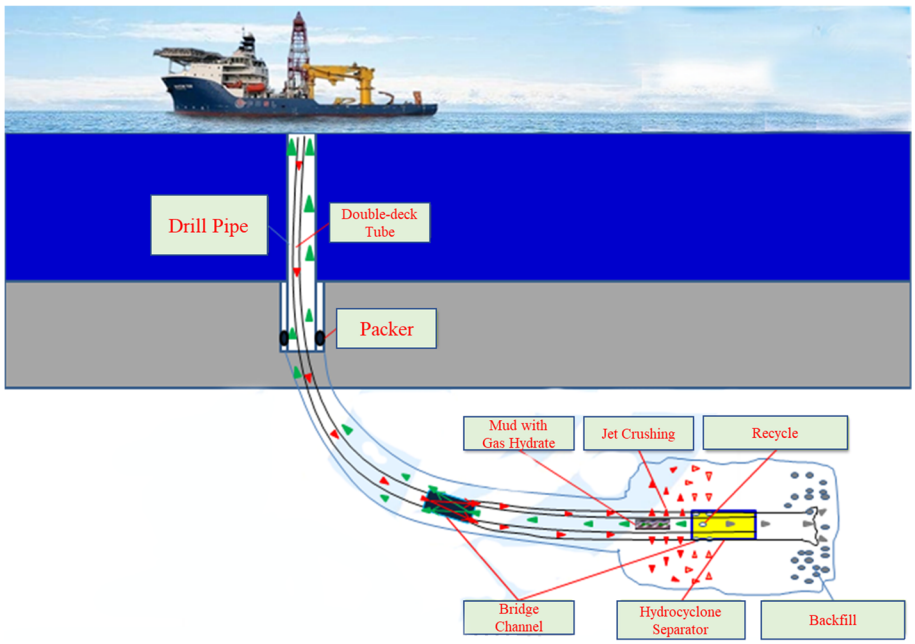

Fig. 1 Technological process for solid fluidization mining of NGH from double-layered pipes [9]

fluidization trial exploitation in the Shenhu Sea, South China Sea, demonstrated the feasibility of the technical principle of the method [7, 8].

On the basis of the principle of solid fluidization mining process, Wang Guorong et al. [9] presented a hydrate solid fluidization mining technology based on dual gradient drilling of double-layer pipe, which drills horizontally and forms a collar hole through a double-layer continuous pipe and a hydrate mining tool (Fig. 1). The advantage of this method is that it converts the dynamic circulation in the bare borehole annulus of traditional drilling into dynamic circulation in the double-layered pipe and transforms the traditional hydrate mining method from uncontrollable to controllable mining, improving the safety of hydrate mining and reducing the risk of engineering and geological disasters in hydrate development. However, the technology still faces problems like low mining efficiency and lack of key equipment, such as the structure of nozzles for water jet crushing has not yet been determined, and the arrangement of jet holes is not optimized.

The use of water jets to crush hydrate reservoirs is a core process in the solid fluidization mining process, but the nozzle structure and nozzle arrangement of the jet tool have not yet been optimized. High-pressure water jets could be classified into various categories, as shown in Table 1. In accordance with the classification criteria, the solid fluidization single-nozzle jet model belongs to single-phase Newtonian fluid free continuous submerged jet.

During the submerged jets process, the jet water will form a free shear surface with the ambient water, and the free shear surface thickness will increase along the water flow direction, and it will become unstable rapidly and form turbulence, and then diffuse to the surroundings to generate adsorption on the ambient water [10]. Figure 2 shows a schematic diagram of the submerged jet structure. As shown in the diagram, the development of the nozzle jet can be generally classified into four

Table 1 Classification of water jets

Classification criteria	Classification categories
Jet characteristics	Single-phase fluid jets, solid-liquid two-phase jets, solid-liquid-gas three-phase jets
Jet media	Non-Newtonian fluid jets, Newtonian fluid jets
Jet environment	Submerged jets, non-submerged jets
Jet generation mechanism	Continuous jets, discontinuous jets
Jet pressure	Low-pressure jet (0∼35 MPa), high-pressure jet (35∼140 MPa), ultra high-pressure jet (> 140 MPa)
Wall conditions	Free jet, non-free jet

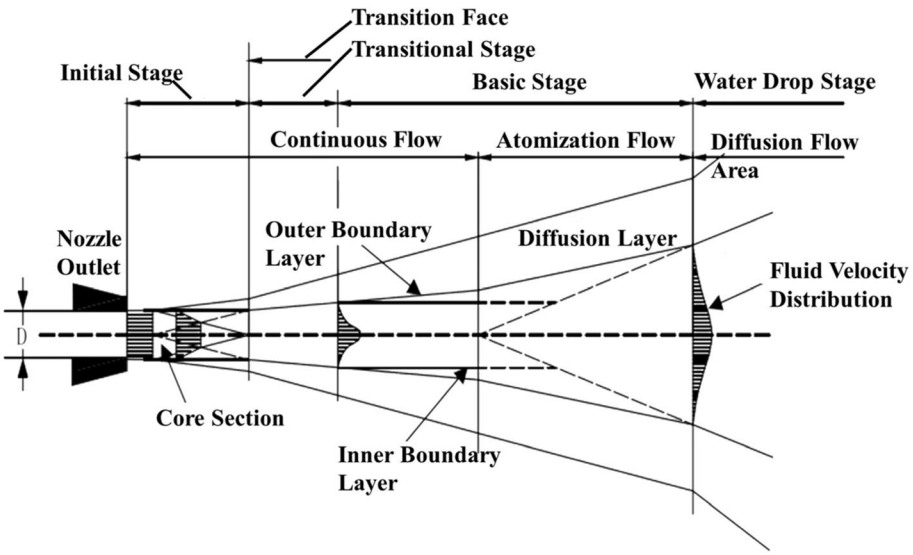

Fig. 2 Schematic diagram of the low pressure submerged jet structure [11]

stages, namely the initial, transition, basic, and water drop stage [11]. In the initial stage, there is a region where the velocity remains constant, called the jet core stage. The jet passes through the turning surface and then enters the jet transition stage, where the jet direction and the magnitude of the velocity change abruptly. As it enters the basic stage of the jet, the axial flow velocity and dynamic pressure values of the jet fall according to a certain pattern and are distributed in a Gaussian curve in the radial area. As the jet process develops, the media velocity and jet flow pressure values become very low, while the jet media and the ambient media will be almost completely integrated in the jet loss area. In practical engineering applications, the utilization of each section of the jet is selected according to different requirements, and to achieve the maximum energy conversion rate and efficiency of use.

The rock breaking mechanism under water jet action has not yet formed a unified theory. The main reason is that the breaking process action time is short, it involved the multi-phase coupling process, and many factors such as jet pressure, nozzle structure, moving speed and action distance need to be considered. And the complex and variable mechanical characteristics of the breaking object also increase the study difficulty. Therefore, the rock breaking process by high-pressure water jet is very complex [12]. At present, there are mainly five theories [13, 14, 15]: ① quasi-static elastic

crushing theory [16, 17]; ② stress wave theory [18]; ③ cavitation rock breaking theory [19, 20, 21, 22]; ④ crack propagation theory [23, 24, 25]; and ⑤ seepage stress and damage fracture theory [26].

Natural gas hydrate deposit is a kind of weakly cemented mineral, and its mechanical properties is significantly different from rock. Therefore, the applicability of the above rock jet fracture theory to hydrate is not clear. Yang Lin [27] divided the hydrate containing sediments crushing process under high-pressure water jet into three stages: ① the water jet makes the surface sediments subject to tensile shear action, and the initial crushing pit appears; ② when the water jet reaches the middle of crushing pit, it expands laterally under the resistance to expand the crushing pit; and ③ after the water jet reaches the bottom of crushing pit, the strength decreases and the expansion speed of the crushing pit decreases.

Shen Juan et al. [28] carried out a study on the design and structural optimization of high-pressure water jet nozzles, and the flow field distribution of five nozzles was analyzed. Li Jingbin et al. [29] conducted a study on the law of influence of parameters such as surrounding pressure, discharge volume, and number of boreholes on jet flow, and analyzed the energy conversion efficiency of porous nozzles, and a rotary jet porous nozzle applicable to radial horizontal well technology was also designed. Liao et al. [30] established a mathematical model of the hydraulic cutting nozzle flow field and obtained the effect of the nozzle contraction angle, nozzle outlet diameter, and cylindrical section length on the jet impact. Ren Fushen et al. [31] researched on jet breaking derived from particle rock breaking and established models for energy conversion efficiency, water in the nozzle and particle acceleration and pressure drop for three types of nozzles. Song et al. [32] studied the internal and external flow fields of four common tapered converging nozzles and found that the jet collection performance and stability of tapered short-line nozzles were better than others. Wang et al. [33, 34] evaluated the breaking effect from shape regularity of broken hole, variation of broken hole diameter, breaking efficiency, and solid phase concentration of slurry formed by the jet. However, there are few existing studies that have investigated the jet effect of nozzles based on the solid fluidization process of double-layered pipes.

To improve the working performance of hydrate solid fluidization mining tools and promote the process of large-scale extraction of marine hydrate in China, this article selected six nozzle structures commonly used for jet flow, and analyzed the axial velocity distribution of nozzle flow field, axial velocity decay law, maximum flow velocity in the outer area and core stage length, and the optimal nozzle structure type for solid fluidization jet crushing process was determined. On the basis of the double-layer piper solid fluidization mining process, the pressure drop and flow resistance coefficients of the double-layer piper annulus with different number of single nozzles, axial nozzle spacing and total number of nozzles were developed, and the optimal multiple nozzle arrangement was obtained, it providing a theoretical basis for the design of the double-layer piper solid fluidization mining tool for marine hydrates.

Flow field analysis for single nozzle submerged jets and nozzle structural optimization

Flow field simulation and modelling

The jet flow characteristics of nozzles is mainly affected by the following four structural parameters: inlet and outlet diameter, cylindrical section length to diameter ratio,

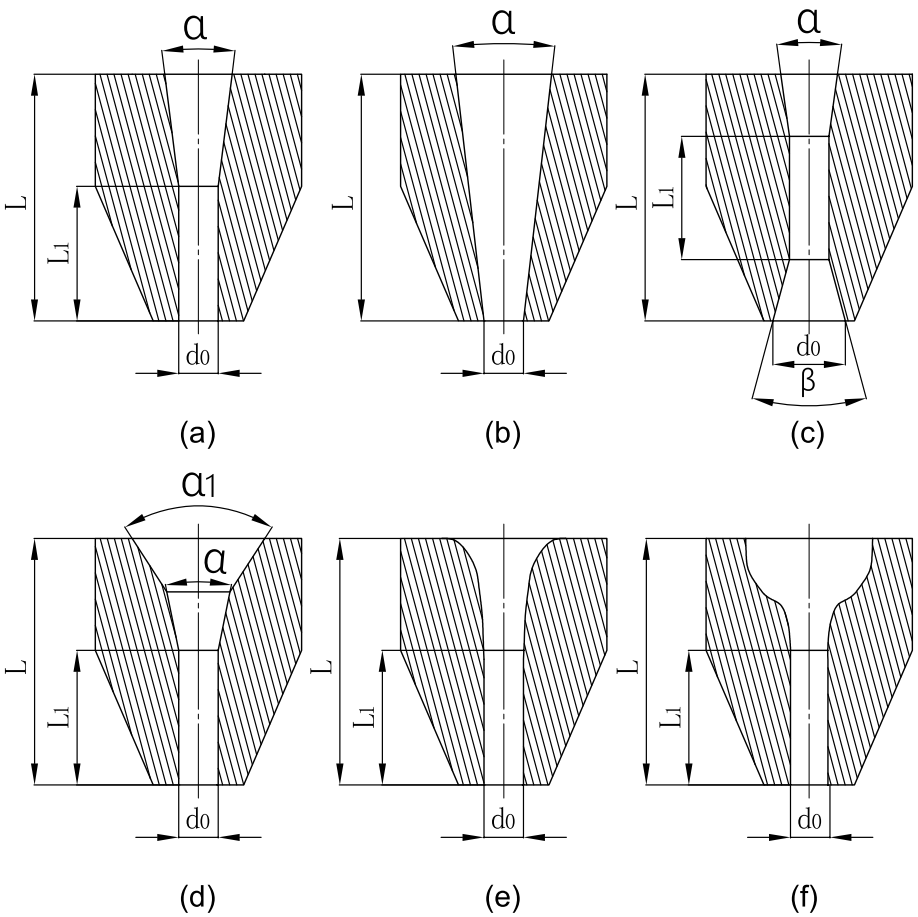

Fig. 3 Common nozzle structures for rock breaking [36]**. a** Straight-taper nozzle. **b** Convergent nozzle. **c** Convergent-divergent nozzle. **d** Dual gradient nozzle. **e** Constant velocity gradient nozzle. **f** Streamline Nozzle

contraction angle, and transition section length [35]. ① Nozzle diameter mainly influences the jet flow velocity and influence range, while nozzle diameter is too large or too small will lead to high energy consumption or easy blockage and other problems, respectively; ② cylindrical section length to diameter ratio and the length of the transition section affect the degree of jet turbulence; ③ contraction angle affects the media flow in the nozzle by the flow resistance and stroke loss.

Single nozzle structures commonly used in rock breaking [36] are shown in the Fig. 3, it mainly including linear nozzles (flat, convergent, straight-taper, etc.), non-linear nozzles (constant velocity gradient, streamlined, elliptical, etc.), and shaped nozzles (fan, star-shaped).

The main design parameters of nozzles include the constriction angle α , the nozzle diameter d_0, the overall nozzle length L, and the nozzle cylindrical section length to diameter ratio L_1/d_0. The double gradient nozzle (d) also involves a first constriction angle α_1, the diffusion nozzle is designed with a diffusion angle β, while the nozzle diameter d_0 can be calculated by following formula: $A = \frac{q}{\mu\sqrt{2Pg}}$. While A is the cross-sectional area of the nozzle (m^2), q is the nozzle flow (m^3/h), μ Is the flow coefficient, g is the gravitational acceleration (m^2/h), P is the working pressure of the nozzle (MPa). Other

parameters can be obtained according to the value of d_0. And the flow path equation for the non-linear section of the isotropic nozzle (e) uses the flow path bus equation [31], and the non-linear section of the streamline nozzle adopts the cosine function as the flow path bus equation. Six nozzle configurations were designed for their dimensions, and the specific parameters of each nozzle structure are described in Table 2.

Simulation models and calculation methods

To optimize the nozzle structure and structural parameters to achieve best jet effect, 3D models for six nozzles were developed and simulations were performed. The model is shown in Fig. 4a and consists mainly of the nozzle structure and the outflow field of the jet. The structure, dimensions, and the boundary condition of the model are shown in Fig. 4b. By adjusting the dimensions of the nozzle, the simulation of all six nozzles can be achieved.

All simulations were performed using the ANSYS FLUENT, and performed based on steady-state and pressure-based conditions. The turbulence model is standard k-ε model, which is mainly applicable to the complete turbulence working condition. The SIMPLE scheme is applied for pressure velocity coupling. The results of the model meshing are displayed in Fig. 5. For the simulation, the model inlet was set to a pressure inlet of 15 MPa and a confining pressure of 10 MPa, and the outlet was set to a pressure outlet.

As seawater is usually used as the jet medium in solid fluidization jet process, it is adopted as the jet medium with material parameters of density 1025 kg/m^3 and viscosity coefficient 0.0017.

Mesh independence validation

To eliminate the effect of mesh number, and chose appropriate mesh number for simulation, the investigations were carried out based on the computational model shown in Fig. 5. The four groups of models with mesh number of 115,646, 219,912, 367,181, and 655,232 are constructed and with same settings shown before. The velocity at the end of inlet was calculated and shown in Fig. 6. The fluid velocity presents a negligible deviation of 0.15% when the mesh number increases from 219,912 to 655,232. To save the computing resources, selected the model with 219,912 mesh for simulation.

Results and discussion

Aiming at the submerged free jet simulation results of six nozzles in Fig. 3, the variation patterns of velocity decay, radial velocity distribution and turbulent kinetic energy of the axial center under different nozzles were compared, so as to select the best structure for the subsequent design analysis of the nozzle dimensions.

Table 2 Structural parameters of the design nozzle

Nozzle type	L	L_1/d_0	α/(°)	α_1/(°)	d_0/mm	β/(°)
a	12	3	13	-	2	-
b	12	-	13	-	2	-
c	12	3	13	-	2	20
d	12	3	60	13	2	-
e	12	3	13	-	2	-
f	12	3	13	-	2	-

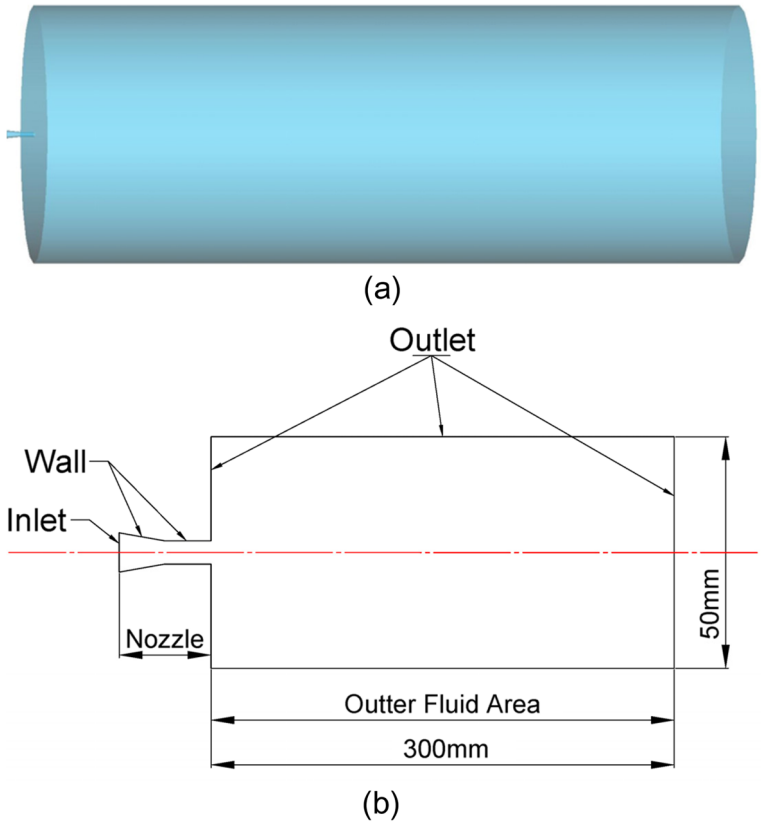

Fig. 4 Single nozzle simulation geometry model

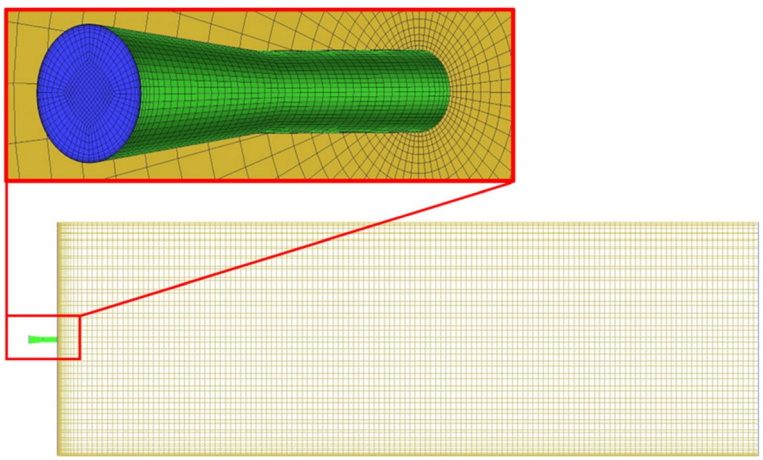

Fig. 5 Single nozzle flow field model meshing. **a** Nozzle structure. **b** Extraction chamber structure. **c** nozzle mesh. **d** Extraction chamber mesh. **e** Overall mesh

Mesh reliability validation

The maximum jet velocity of six nozzles is shown in Fig. 7. According to the empirical formula, the theoretical maximum jet velocity of the nozzle is calculated by the formula $u_{\max} = 44.7\sqrt{P_t}$, while P_t is the total pump pressure. According to the

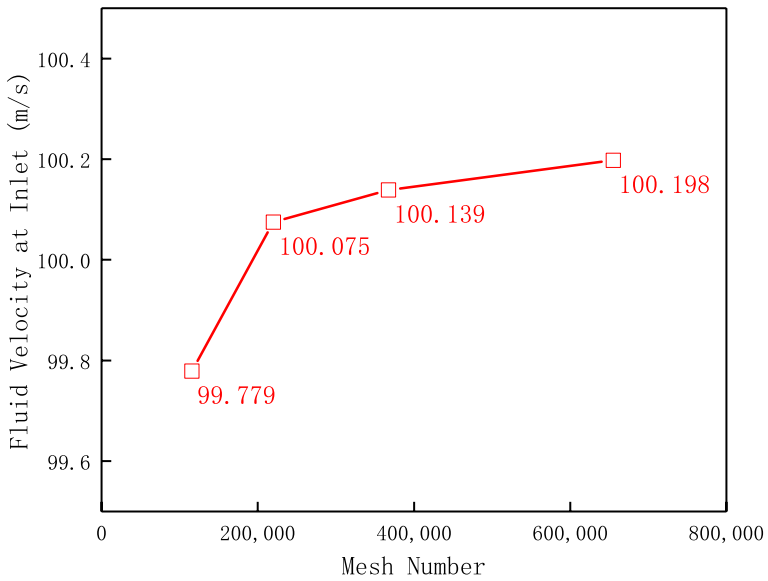

Fig. 6 The indicator velocity with different mesh numbers

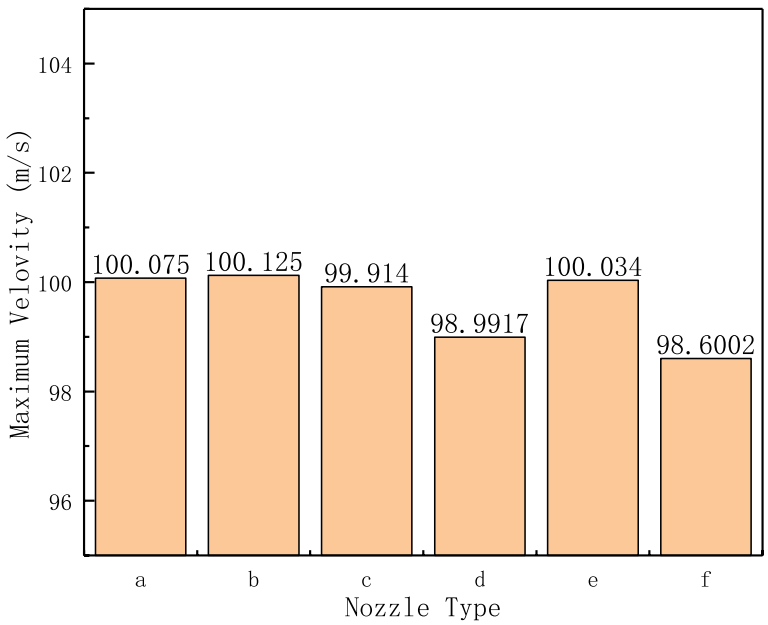

Fig. 7 Maximum outlet velocity for six nozzle configurations

simulation setting, the u_{max} should be about 99.952 m/s. Comparing u_{max} with the value in Fig. 7, all errors are less than 1.5%. Therefore, the simulation method adopted is feasible.

Axial velocity distribution

Figures 8 and 9 respectively show the velocity cloud charts at the flow path and outlet of six nozzles. As it shows, the velocity field from different nozzle jet has a similar

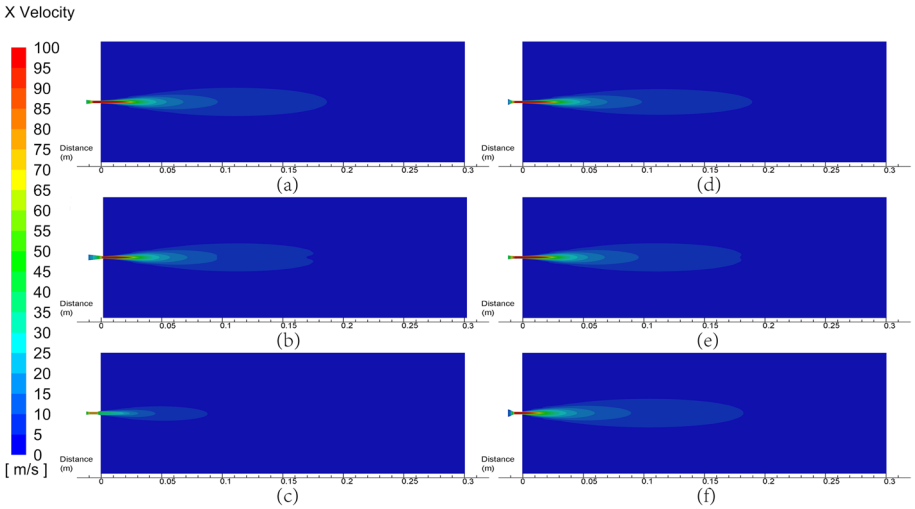

Fig. 8 Velocity cloud of different nozzle configurations. **a** Straight-taper nozzle. **b** Convergent nozzle. **c** Convergent-divergent nozzle. **d** Dual gradient nozzle. **e** Constant velocity gradient nozzle. **f** Streamline Nozzle

trend, that the fluid medium reached the maximum velocity after contracting in the contraction stage, i.e., the jet has the maximum flow. Subsequently, the fluid through the cylindrical section and become stabilize, it enters the outer area; the jet leaves the nozzle outlet, the divergence phenomenon begins to appear. Meanwhile, the jet velocity gradually decays due to the influence of the outer area resistance, presenting a "pointed cap" Gaussian distribution in the outer area.

The outer area velocity field distribution shows that ① the dissipation section of nozzle (c) is longer and the jet diffusion is larger, but the energy concentration is poor, so when it used to crushes, the phenomenon of a large crushing diameter and small crushing depth would occur, the concentration of its crushing effect is significantly worse than the others. ② The core stage of nozzle (c) and nozzle (f) is smaller than the others, which means that the performance of nozzle © and (f) were the worst. ③ In terms of overall water jet development, nozzle (a) and (e) have more stable jets and less energy dissipation, and are more conducive to the hydrates jet crush. Furthermore, the jet velocity distributions of nozzles (a–d) are generally relatively similar.

Decay of axial velocity

Figure 10a shows the velocity distribution along the central axis of six nozzles. As it shows, the fluid velocity in the five types of nozzles in addition to the nozzle (c) has a similar pattern. After fluid enters the nozzle, the axial velocity is linear growth; when the fluid leaves the nozzle, the axial velocity decreases rapidly. When the fluid is inside the nozzle (c), the axial velocity grows rapidly and then immediately decay quickly, its axial velocity maximum value reaches others about 1.7 times. But at the nozzle outlet position, the speed will decay to a similar range with other nozzles.

As Fig. 10a shows, the velocity magnitude at the nozzles' outlet is similar, and the fluid axial velocity above 50 mm from the nozzle outlet is not met jet crushing condition. Therefore, it can be judged that the key of nozzle efficiency is focused on the range of 0–50 mm outside the nozzle. Nozzle outlet and 50 mm from it at the velocity decay

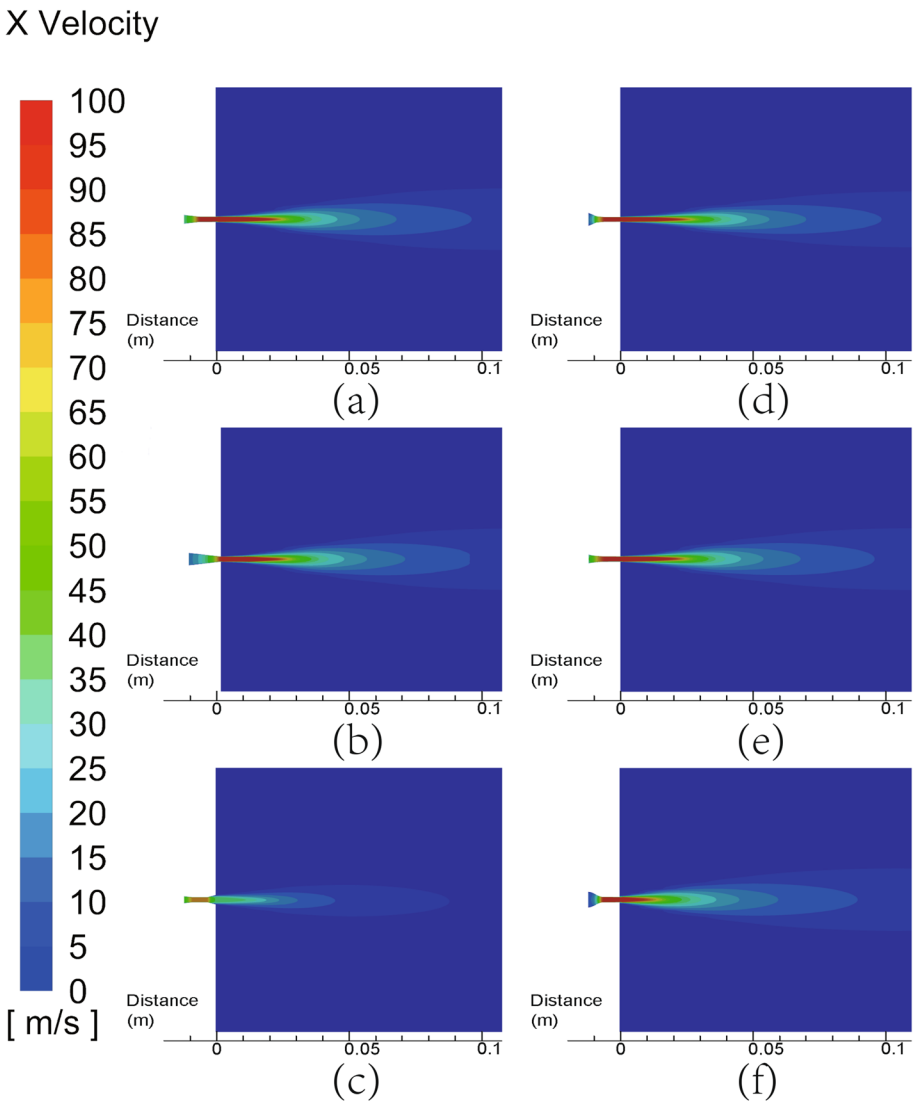

Fig. 9 Velocity cloud at the outlet of the jet with different nozzle configurations. **a** Straight-taper nozzle. **b** Convergent nozzle. **c** Convergent-divergent nozzle. **d** Dual gradient nozzle. **e** Constant velocity gradient nozzle. **f** Streamline Nozzle

was intercepted for analysis, and the results are shown in Fig. 10b. From Fig. 10b, fluid axial velocity of nozzle (c) and (f) decay faster, the axial velocity at 50 mm is significantly lower than the others. Fluid axial velocity decay rate and the difference between the fluid axial velocity of other nozzles at 50 mm are smaller. And the fluid axial velocity of nozzle (b) was the smallest at the outlet, and it continued increase with the jet until it reached the maximum value. Nozzle (a), (d), and (e) have similar fluid filed change pattern, with a flat section after the nozzle outlet and then begin to decay swiftly.

According to Wang's [33, 34] calculation model of hydrate breaking rate, the size of hydrate breaking pit is highly related to the critical fluid velocity and hydrate saturation, and it increases with the increase of critical fluid velocity. Consequently, the structures

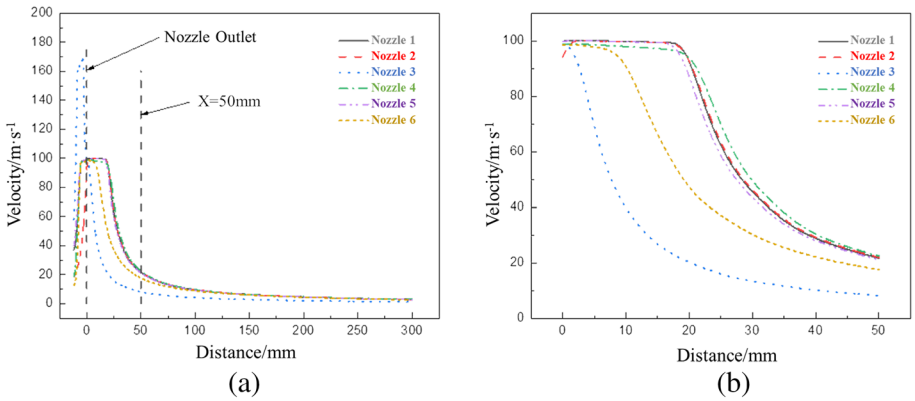

Fig. 10 Axial velocity decay of the jet fluid for different configurations of nozzles. **a** Axial spacing range 0–300 mm. **b** Axial spacing range 0–50 mm

of nozzle (a), nozzle (b), nozzle (d), and nozzle (e) should be preferred over nozzle (c) and nozzle (f).

Length of core stage

Figure 11 shows the core stage length of each nozzle jet. Longer jet core stage and jet energy concentrated stage are more favorable for the NGH jet crushing. As shown in Fig. 11, nozzles (a), (e), and (b) have the longest jet core stage, approximately 18 mm, 17 mm, and 16 mm respectively. Nozzles (d) and (f) have a much shorter core stage length, both below 10 mm. And the core jet stage length of nozzle (c) is almost zero because of the shrinkage section. Therefore, nozzle (a) is the best structure among the six nozzles.

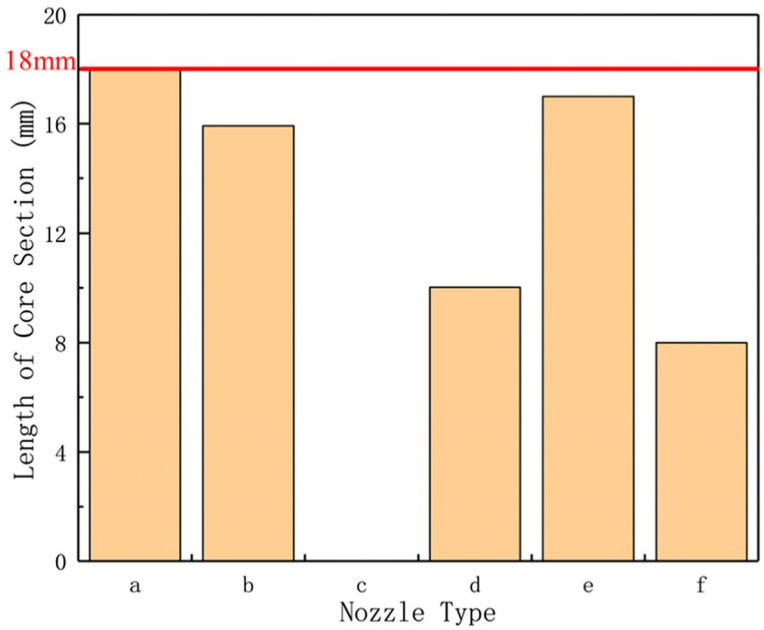

Fig. 11 Length of the core stage of each nozzle jet

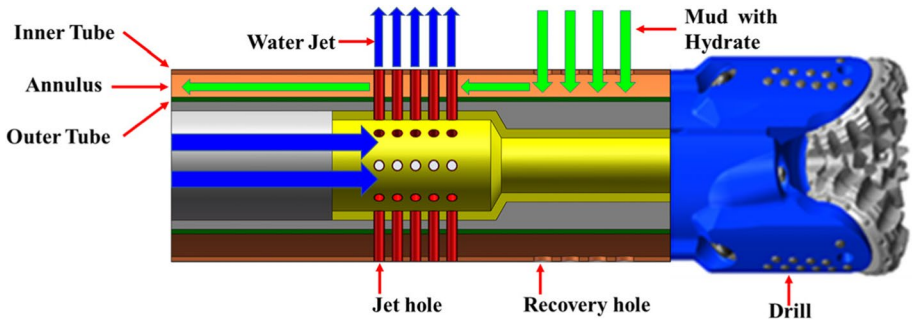

Fig. 12 Schematic diagram of the solid fluidization tool for double-layer pipe

Therefore, nozzle (a) and (e), compared to other nozzles, have the advantage of a more stable jet, better axial velocity distribution of the internal fluid and high axial velocity of the fluid at the outlet. Also, nozzle (a) has a slightly longer core stage length than nozzle (e). So, nozzle (a) was chosen to be used for solid fluidization jet crushing of hydrates.

Design analysis of nozzles arrangement and axial spacing

Flow field modelling and simulation

Figure 12 shows the structure of a double-layer pipe solid fluidization tool. In the solid fluidization mining process based on dual gradient drilling of double-layer pipe, the jet holes are required to occupy the hydrate slurry transport channel, i.e., the outer annular void of the double-layer pipe, and affect the channel over-flow performance. Therefore, the study of the jet hole arrangement for multi-hole water jet has important implications for the solid fluidization tool design. After completing the optimization of the nozzle structure, combined with the results of the single-nozzle jet crushing law study [37] and the crushing depth prediction model study [38], the

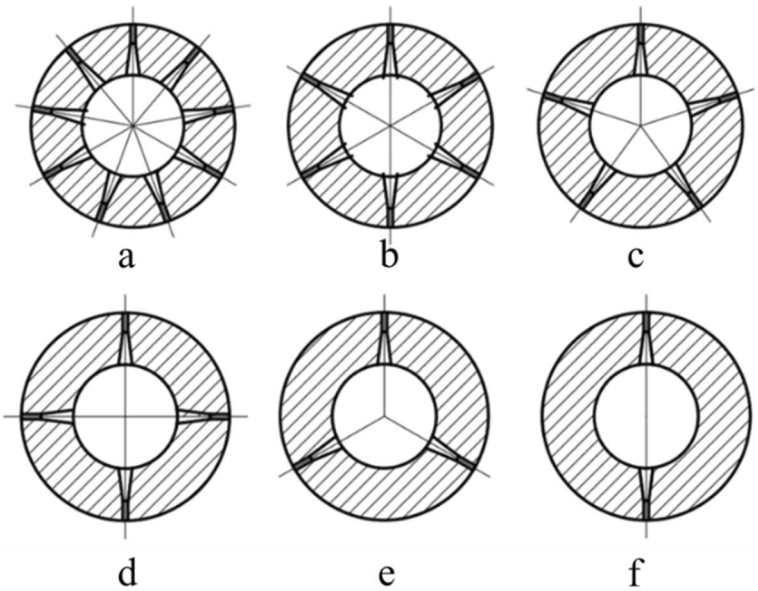

Fig. 13 Six nozzle arrangements. Number of nozzles in a single circle: **a** 9, **b** 6; **c** 5; **d** 4; **e** 3; **f** 2

Table 3 Experimental scheme for simulation and analysis of layout

No.	Total number of nozzles	Arrangement	Axial spacing (mm)	No.	Total number of nozzles	Arrangement	Axial spacing (mm)
1	12	f	25	11	15	e	75
2	12	e	25	12	15	c	25
3	12	d	25	13	18	f	25
4	12	b	25	14	18	e	25
5	12	e	15	15	18	b	25
6	12	e	50	16	18	a	25
7	12	e	75	17	18	e	15
8	15	e	15	18	18	e	50
9	15	e	25	19	18	e	75
10	15	e	50	-	-	-	-

influence analysis of nozzles number and axial spacing between nozzles on the over-flow performance of the double-layer pipe annulus in the dual gradient double-layer pipe solid fluidization process was investigated.

When the jet flow rate and nozzle diameter is fixed, the main factors affecting the jet crushing efficiency are the nozzles number and the arrangement. When optimizing the nozzle arrangement, the impact of the axial spacing between two nozzles and the number of nozzles in same circle should be considered primarily.

To select the best multiple nozzles arrangement, research of nozzle arrangement were carried out. The total nozzles number was selected as 12, 15, and 18, nozzles number in the same circle was selected as 2, 3, 4, 5, 6, and 9; the axial spacing was selected as 15, 25, 50, and 75 mm. Based on that, six nozzle arrangements were designed as shown in Fig. 13. Furthermore, 19 sets of simulation experimental scenarios were obtained by combining different nozzle counts and nozzle axial spacing, as presented in Table 3.

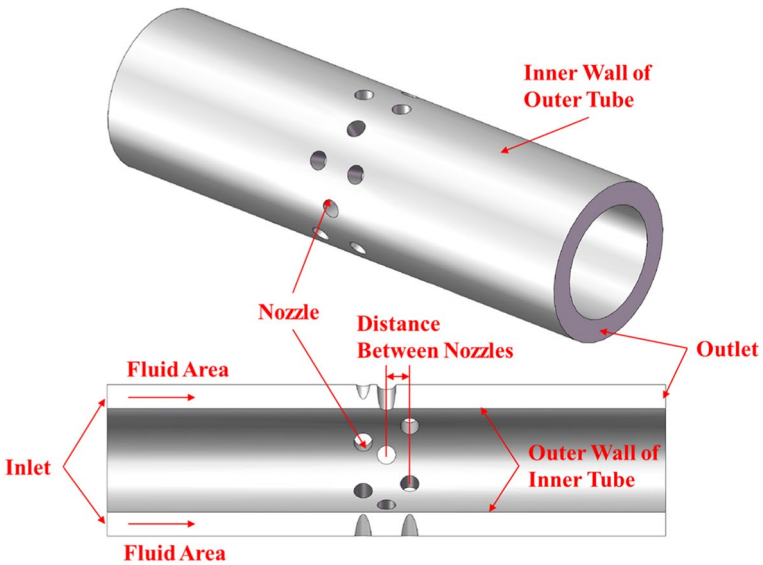

Fig. 14 Simulation model for the analysis of the jet device outer annulus over-flow performance

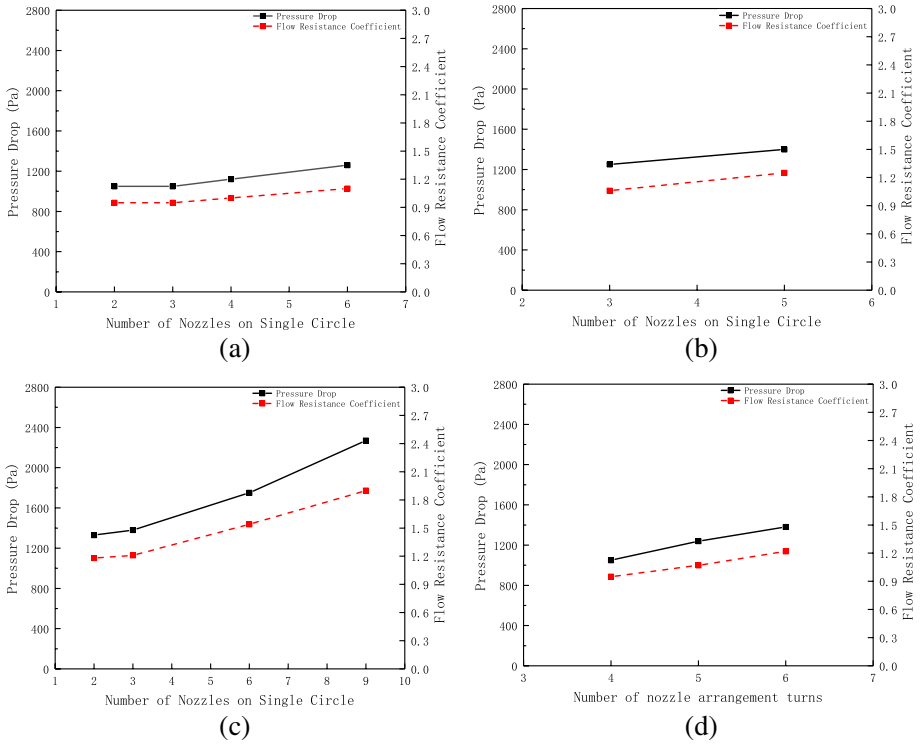

Fig. 15 Variation of fluid pressure drop and flow resistance coefficient with nozzle arrangement in the outer annulus. Total number of nozzles: **a** 12, **b** 15, **c** 18; **d** number of nozzle circles

Simulation model and calculation method

Based on the above arrangement, the simulation geometry model shown in Fig. 14 was developed. The model consists of an annular flow path formed by the inner and outer pipe of the double-layer pipe, the outer wall surface of the single nozzle, inlet, and outlet. In particular, the outer wall of the inner pipe, the inner wall of the outer pipe and the outer surface of the nozzle were formed as non-slip wall surface of the model. The boundary conditions are velocity inlet and free flow outlet. The annular inlet velocity is derived from the nozzle flow rate and is approximately 1.5 m/s. As the double-layer pipe hydrate slurry flow condition is close to a circular pipe disturbance, the k-ε standard model is selected for the solution. And the SIMPLE algorithm was adopted for the general solution to reduce the computational effort. Considering the influence of hydrate on the slurry parameters, the density of NGH is 910 kg/m^3, assume that the hydrate saturation in the slurry is 25%, so the density of NGH mud is 996.25 kg/m^3.

Results and discussion

Number of nozzles in the same circle

Figure 15 shows the relationship between the fluid overflow pressure drop and the flow resistance coefficient of the outer annulus with the nozzle arrangement. Figure 15a–c shows that as the number of nozzles in same circle increases, the pressure drop and flow resistance coefficient of the outer annulus fluid gradually increases. In other words, the greater the number of nozzles in same circle arranged, the smaller the over-flow area

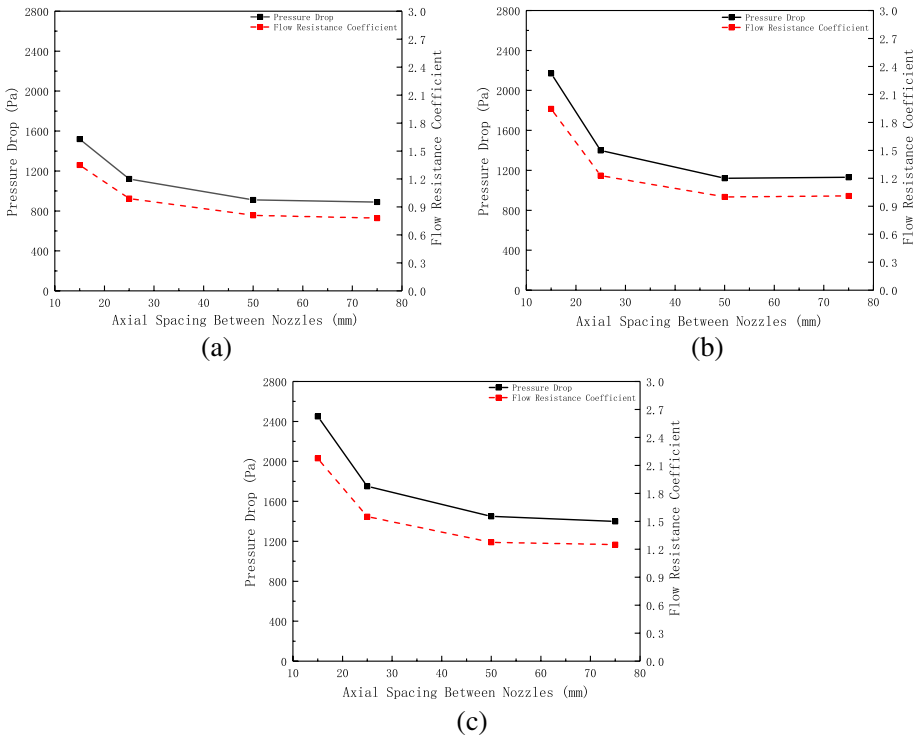

Fig. 16 Relationship between outer annulus pressure drop and flow resistance coefficient with axial spacing. Total number of nozzles is **a** 12, **b** 15, **c** 18

in the same cross-section, and the greater the obstruction to fluid passage, which will directly reduce the hydrate slurry transport efficiency. In addition, with the increase of the number of nozzles in the same circle, the more the total number of nozzles, the faster the fluid pressure drop and flow resistance coefficient increase. It is because that more nozzle circles will affect the fluid passage efficiency many times. And to increase the annular flow performance, the total nozzles number and the number of nozzles in the same circle should be limited while ensuring the water jet effect. Comparing Fig. 15a and c, the change in pressure drop and flow resistance coefficient is smaller when the number of nozzles in the same circle is 2 and 3. As Fig. 15d shows, when the number of nozzles in the same circle is the same, the pressure drop and flow resistance coefficient of the outer annular fluid becomes larger with the increase in the number of nozzles circles.

Axial spacing

In consideration of when the number of nozzles in the same circle being 2, or the axial spacing of nozzles are too large, the range of jet influence may be insufficient. Therefore, it is recommended that the number of nozzles in the same circle is 3 and the axial spacing between nozzles is approximately 50 mm.

Total number of nozzles

In comparison with Figs. 15 and 16, it can be found that when the nozzle arrangement is the same, as the total number of nozzles increases, the pressure drop and flow resistance

coefficient in the ring air also increases. If the number of nozzles in the same circle is 3, and the total number of nozzles is 12, the pressure drop is about 1050 Pa, the flow resistance coefficient is about 0.95. When the total number of nozzles increases to 15 and 18, the pressure drop increases by 19.5% and 28.57% respectively, and the flow resistance coefficient increases by 11.58% and 27.39% respectively. When the nozzle axial spacing is 50 mm and the total number of nozzles is 12, the pressure drop is about 910 Pa, and the flow resistance coefficient is about 0.81. When the total number of nozzles increases to 15 and 18, the pressure drop increases by 23.08% and 56.84% respectively, and the flow resistance coefficient increases by 19.12% and 57.41% respectively. Therefore, to ensure the jet effectiveness, it is necessary to reduce the total number of nozzles as much as possible to achieve a better over-flow performance in the extraction loop. Under the current study conditions, the recommended total number of nozzles is 12.

In view of the results, it is recommended that the multi-nozzle arrangement used for the solid fluidization tool with: the number of nozzles in a single circle is 3, the axial spacing between nozzles is 50 mm and the total number of nozzles is 12.

Conclusions

To optimize nozzle configuration for the hydrate solid fluidization mining technology, and investigate the nozzle arrangement for hydrate slurry overflow performance in double-layer pipe annulus under the influence of multiple nozzles, based on Fluent, single-nozzle jet flow analysis of various configurations was undertaken, and the overflow performance in double-layer pipe annulus under various multiple nozzle arrangements was compared, and the following conclusions were obtained:

(1) The jet energy diffusion of the convergent-divergent nozzle is the fastest, the outlet axial velocity is the smallest, and the core stage length is almost zero. Straight-taper nozzle and constant velocity gradient nozzle have the best performance in the fluid axial velocity distribution and axial velocity, while the core stage of the straight-taper nozzle length is the largest. Therefore, the straight-taper nozzle is the most suitable nozzle type for hydrate jet crushing.
(2) When the number of nozzles in the same circle is no more than 3 and the axial spacing between the nozzles is not less than 50 mm, the double-layer pipe annulus had the best overflow performance. And the more the total number of nozzles, the worse the over-flow performance of the double-layer pipe annulus.
(3) When designing a solid fluidization jet tool, it is recommended to use a straight-taper nozzle with 3 nozzles in the same circle, 50 mm axial spacing between nozzles and 12 total number of nozzles.

Abbreviation

NGH Natural gas hydrate

Acknowledgements

We would like to acknowledge the support and guidance from Professor Wang Guorong and Zhang Jichun during this research work.

Authors' contributions
All authors contributed to the manuscript and have read and approved the final version. FXY provides the theme and innovation of this article. ZL performed the numerical simulation. FXY, LX, and ZL were responsible for the analysis. FX and ZL were responsible for the writing the manuscript. LJ performed the revisions. All authors read and approved the final manuscript.

Funding
This research is financially supported by the National Key Research and Development Program of China (Nos. 2019YFC0312305 and 2016YFC0304008); Southern Marine Science and Engineering Guangdong Laboratory (Zhanjiang) (No. ZJW-2019-03)

Availability of data and materials
The datasets generated during and/or analyzed during the current study are available from the corresponding author on reasonable request.

Declarations

Competing interests
The authors declare that they have no competing interests.

Received: 11 June 2022 Accepted: 12 September 2022
Published online: 23 October 2022

References

1. Wu NY, Zhang GX, Liang JQ (2013) Progress of gas hydrate research in Northern South China Sea. Adv New Renew Energ 1(1):80–94
2. Chong ZR, Yang SHB, Babu P et al (2016) Review of natural gas hydrates as an energy resource: Prospects and challenges. Appl Energy 162:1633–1652
3. Liu W, Li Y, Xu X (2019) Influence factors of methane hydrate formation from ice: Temperature, pressure and SDS surfactant. Chin J Chem Eng 27(2):405–410
4. Makogon YF (2010) Natural gas hydrates -a promising source of energy. J Nat Gas Sci Eng 2(1):49–59
5. Milkov AV (2004) Global estimates of hydrate-bound gas in marine sediments: how much is really out there. Earth-Sci Rev 66(3-4):183–197
6. Shouwei Z, Wei C, Qingping L (2014) Deep water and shallow natural gas hydrate solid fluidization green mining technology. China Offshore Oil Gas 26(5):7
7. Shouwei Z, Jinzhou Z, Qingping L et al (2017) Optimal design of the engineering parameters for the first global trial production of marine natural gas hydrates through solid fluidization. Nat Gas Ind 37(9):1–14
8. Guorong W, Rong H, Lin Z et al (2018) An optimal design of crushing parameters of Marine gas hydrate reservoirs in solid fluidization exploitation. Nat Gas Ind 10:84–89
9. Guorong W, Lin Z, Qingyou L et al (2019) Research on marine petroleum and hydrate development technology based on dual gradient drilling of double-layer pipe. Ocean Eng Equip Technol 6(S1):225–233
10. Soyama H, Saito K, Saka M (2002) Improvement of fatigue strength of aluminum alloy by cavitation shotless peening. J Eng Mater Technol 124(2):135–139
11. Shengxiong X, Wangping H, Wenwen C (1998) High pressure water jet technology and its application. ChinaMachine Press, Beijing
12. Ruihe W (2010) Study on rock breaking mechanism of high pressure water jet. China University of Petroleum Press, Beijing, p 248
13. Hualin L, Gengsheng L, Can Y (2005) Advance in study on theory of rock breaking under water jet impact. Metal Mine 34(7):1–5, 66
14. Ruihe W, Hongjian N (2003) Theoretical study on rock break-off process during high-pressure water jet drilling. J Univ Petrol 27(4):44–47
15. Forman SE, Secor GA (1974) Mechanics of rock failure due to water jet impingement. Soc Petrol Eng J 14(1):10–18
16. Wang X (2011) Study of Mechanism of Smooth Blasting Combined with Water Jets Slotting in Soft-rock and Its Experiment. Chongqing University, Chongqing
17. Yang J (1997) Theoretical and experimental study on rock breaking mechanism of high pressure water jet. China University of Petroleum, Beijing
18. Xue YXY, Si HSH, Hu QHQ (2017) The propagation of stress waves in rock impacted by a pulsed water jet. Powder Technol 320(10):179–190
19. Stavropoulos Vasilakis E, Kyriazis N, Koukouvinis P et al (2019) Cavitation induction by projectile impacting on a water jet. Int J Multiphase Flow 114(3):128–139
20. Peng KPK, Tian STS, Li GLG et al (2018) Mapping cavitation impact field in a submerged cavitating jet. Wear 396(1):22–33
21. Fujisawa N, Fujita Y, Yanagisawa K et al (2018) Simultaneous observation of cavitation collapse and shock wave formation in cavitating jet. Exp Thermal Fluid Sci 94:159–167
22. M. K K. (2000) The use of cavitating jets to oxidize organic compounds in water. J Fluids Eng 122(3):465–470
23. Ren F, Fang T, Cheng X (2020) Study on rock damage and failure depth under particle water-jet coupling impact. Int J Impact Eng 139:103504
24. Su D, Kang Y, Yan F et al (2018) Crack propagation law affected by natural fracture and water jet slot under blast loading. Combustion, Explosion, Shock Waves 54(6):747–756
25. Birger I, Balepina T (1991) The mechanism and kinetics of propagation—low cycle fatigue cracks in the components of jet engine. Fracture of Engineering Materials and Structures. Springer, Dordrecht, p 711–713

26. Wang L (2015) Study on Mechanism of jet perforation fracturing in horizontal wells. China University of Petroleum (East China), Qingdao
27. Yang L (2018) Study on the breaking process of marine hydrate reservoirs subjected to high pressure water jet and the production increase of marine hydrate reservoirs reconstruction. Jilin University, Changchun
28. Juan S (2014) High pressure water jet nozzle design and structure optimization. Suzhou University, Suzhou
29. Li Jinbin，Li Gensheng，Huang Zhongwei, et al. Energy conversion efficiency of the multi-orifice nozzle. Fluid Machine, 2017,45(1): 20-25,54.
30. Wentao L, Xiaoyu D (2017) Study on flow field characteristics of nozzle water jet in hydraulic cutting. IOP Conf Ser: Earth Environ Sci 81:012167
31. Fushen R, Tiancheng F, Xiaoze C (2018) Parameter optimization and experimental study of particle jet impact rock breaking nozzle. Petrol Machine 2:5–11
32. Gaofeng S, Hongxiang Z, Yining W et al (2019) Finite element analysis of nozzle selection based on high pressure water jet technology. IOP Conf Ser: Earth Environ Sci 267(4):042053
33. Wang L, Wang G, Mao L et al (2019) Experimental research on the breaking effect of natural gas hydrate sediment for water jet and engineering applications. J Petrol Sci Eng 184:106553
34. Wang L, Wang G (2020) Experimental and theoretical study on the critical breaking velocity of marine natural gas hydrate sediments breaking by water jet. Energies 13(7):1725
35. Baozhen Z (2003) Experimental study on needle-shape nozzle structure affect on its jet characteristics. Tianjin University of science and technology, Tianjin
36. Kang C, Liu H, Yang M et al (2016) Foundation and application of high-pressure water jet technology. Machinery Industry Press, Beijing
37. Jichun Z, Lin Z, Guorong W et al (2021) Experimental study on crushing law of single jet for non-diagenetic gas hydrate. J Central South Univ (Sci Technol) 52(02):607–613
38. Xingyong Y, Lin Z, Guorong W et al (2022) A new model for predicting hydrate breaking depth of single nozzle in solid fluidization exploitation and its verification. Nat Gas Ind 42(03):150–158

Publisher's Note

Springer Nature remains neutral with regard to jurisdictional claims in published maps and institutional affiliations.

Submit your manuscript to a SpringerOpen journal and benefit from:

- ► Convenient online submission
- ► Rigorous peer review
- ► Open access: articles freely available online
- ► High visibility within the field
- ► Retaining the copyright to your article

Submit your next manuscript at ► springeropen.com